Palaeontologia Electronica
palaeo-electronica.org

Ambergris cololites of Pleistocene sperm whales from central Italy and description of the new ichnogenus and ichnospecies *Ambergrisichnus alleronae*

Paolo Monaco, Angela Baldanza, Roberto Bizzarri, Federico Famiani, Marco Lezzerini, and Francesco Sciuto

ABSTRACT

Ambergrisichnus alleronae igen. et isp. nov. from early Pleistocene clay marine deposits of Umbria, central Italy is here described, and attributed to cololites (evisceralites) of sperm whales. This interpretation is supported by the following characteristics that are frequently identified in modern ambergris including: internal organization of concentric structures, external shape with converging striae and bulges (*rognons*), and inclusions of squid beaks. These cololites were deposited in a relatively deep (100-150 m) marine environment, and the large number of structures in a restricted area is plausibly ascribed to multiple death events of sperm whales. The description of *A. alleronae* igen. et isp. nov. is held by analysis of the taphonomic processes that took place after the sperm whale carcasses reached the seabed and led to fossilization. The analysis of benthic micro- and macrofauna found close to the studied structures provides supplementary data, which support the reconstruction of palaeoecological and palaeoenvironmental conditions comparable with those of the whale fall communities. This work increases knowledge of vertebrate coprolites. Moreover, this new information provides the data about the frequency of sperm whales in the Tyrrhenian Sea during the early Pleistocene, and raises new questions about the causes of this anomalous accumulation.

Paolo Monaco. Department of Physics and Geology, University of Perugia, Via Pascoli – I-06123 Perugia, Italy. paolo.monaco@unipg.it
Angela Baldanza (corresponding author). Department of Physics and Geology, University of Perugia, Via Pascoli – I-06123 Perugia, Italy. angela.baldanza@unipg.it
Roberto Bizzarri. Department of Physics and Geology, University of Perugia, Via Pascoli – I-06123 Perugia, Italy. roberto.bizzarri@libero.it
Federico Famiani. School of advanced studies–Geology division, University of Camerino, Via Gentile III da Varano – I-62032 Camerino, Italy. federico.famiani@unicam.it
Marco Lezzerini. Department of Earth Sciences, University of Pisa, Via Santa Maria, 53 – I-56126 Pisa, Italy. marco.lezzerini@unipi.it

http://zoobank.org/BC6FAF96-D292-4A5D-A2D0-3A6797185E81

PE Article Number: 17.2.29A

Submission: 27 February 2014. Acceptance: 24 July 2014

Monaco, Paolo, Baldanza, Angela, Bizzarri, Roberto, Famiani, Federico, Lezzerini, Marco, and Sciuto, Francesco. 2014. Ambergris cololites of Pleistocene sperm whales from central Italy and description of the new ichnogenus and ichnospecies *Ambergrisichnus alleronae*. *Palaeontologia Electronica* Vol. 17, Issue 2;29A; 20p;
palaeo-electronica.org/content/2014/824-ambergrisichnus-alleronae

Francesco Sciuto. Department of Biological, Geological and Environmental Sciences, University of Catania, Via A. Longo, 19 – I-95125 Catania, Italy. fsciuto@unict.it

Keywords: Ichnology; Cololites; Sperm whales; early Pleistocene; Palaeoenvironment; Central Italy, ichnogenus; ichnospecies

INTRODUCTION

The term coprolite (from the Greek *kopros*, dung, and *lithos*, stone) was applied to any type of fossilized digestive material, regardless of origin, since William Buckland coined the term in 1829, but now restricted to material ejected from the posterior of the digestive tract (see etymology in Bromley, 1990; Hasiotis et al., 2007; Hunt and Lucas, 2012a). They are considered bromalites, along with cololites, regurgitalites and other trace fossils (Hunt and Lucas, 2012a). Bromalites are commonly studied in continental environments, where dinosaurs have received the most attention because of their size and possible inferences about their diets (Chin et al., 1998; Piperno and Sues, 2005; Prasad et al., 2005). However, bromalites of other types of vertebrates are known, ranging widely in size, shape and abundance (Hunt, 1992; Spencer, 1993; Hunt et al., 1994; Hunt and Lucas, 2012b). Related trace fossils are classified in a variety of ways including feeding traces (e.g., bite marks and degradation of bones for ingestion) (Duffin, 1979; Hunt, 1992; Hunt et al., 1994; Northwood, 2005; Hasiotis et al., 2007). Cololites are fossilized digestive material preserved in the digestive tract posterior to the stomach (Hunt and Lucas, 2012a), in particular show a range of degradation depending on the degree of digestion before preservation, and the identification of cololites is difficult, but not impossible, unless they are fossilized within the intestinal region of animals (Hunt, 1992, Hunt et al., 2012; Hunt and Lucas, 2012a). Bromalites, meaning ‘‘food stones’’, are defined as any fossilized digested matter originating from animals. Evidence cited in support of a fecal origin may include an extruded shape, variation in shape corresponding to viscosity variations seen in modern specimens, limited length or quantity of material, and striations caused by anal extrusion (Amstutz, 1958; Shelton, 2013). Fossil bromalites of cetaceans were previously unknown. Notably, fossilized ambergris, which represents the most distinctive among all kinds of fecal matter of sperm whales, had never been recognized until the work of Baldanza et al. (2013) on the Bargiano section (southwestern Umbria, northern Apennine, Italy; Figures 1, 2). Preliminary results refer these structures to intestinal products of sperm whales living between 1.75 and 1.55 Ma, and they represent the only known example of sperm whale coprolites. In the same area, north from the Allerona railway station and not far from the Bargiano site, minor ichnofossiliferous horizons have been identified throughout the Montemoro section (Figures 1, 2). The purposes of this paper are an ichnological description, the proposal of the new ichnogenus and the new ichnospecies *Ambergrisichnus alleronae*, and a geologic, stratigraphic, sedimentological, and mineralogical characterization of cololites and of enclosing sediments.

GEOLOGICAL AND STRATIGRAPHIC OVERVIEW

The study area (Figure 1.1) is located in western Umbria (central Italy), about 10 km north of Orvieto, close to the town of Allerona, within the South Valdichiana Basin - a wide extensional basin evolved from the late Miocene onward. The Allerona sector belongs to the Paglia graben, a NW-SE oriented extensional basin bordered by Mesozoic – Cenozoic highlands (the Mt. Peglia/Narnese-Amerina chain, due east, and the Rapolano-Mt. Cetona ridge, due west). Since its evolution began during the early Pliocene, the Paglia graben mainly held a river-fed coastal marine sedimentation from late Pliocene to early Pleistocene (Ambrosetti et al., 1987; Mancini et al., 2004; Baldanza et al., 2011, 2013). Sediments vary from gravels and sands to silty clay deposits, both across and along the paleoshorelines, delineating a very digitate coastal environment. Still, most of deposits cropping out in the Allerona area are gray-blue, massive to thinly laminated offshore marine silty clay. All these deposits are referred to the Chiani-Tevere sedimentary cycle (Gelasian-Calabrian: Ambrosetti et al., 1987; Mancini et al., 2004; Baldanza et al., 2011). Two ichnofossil sites, the Montemoro and Bargiano sections, are described herein (Figure 1.2).

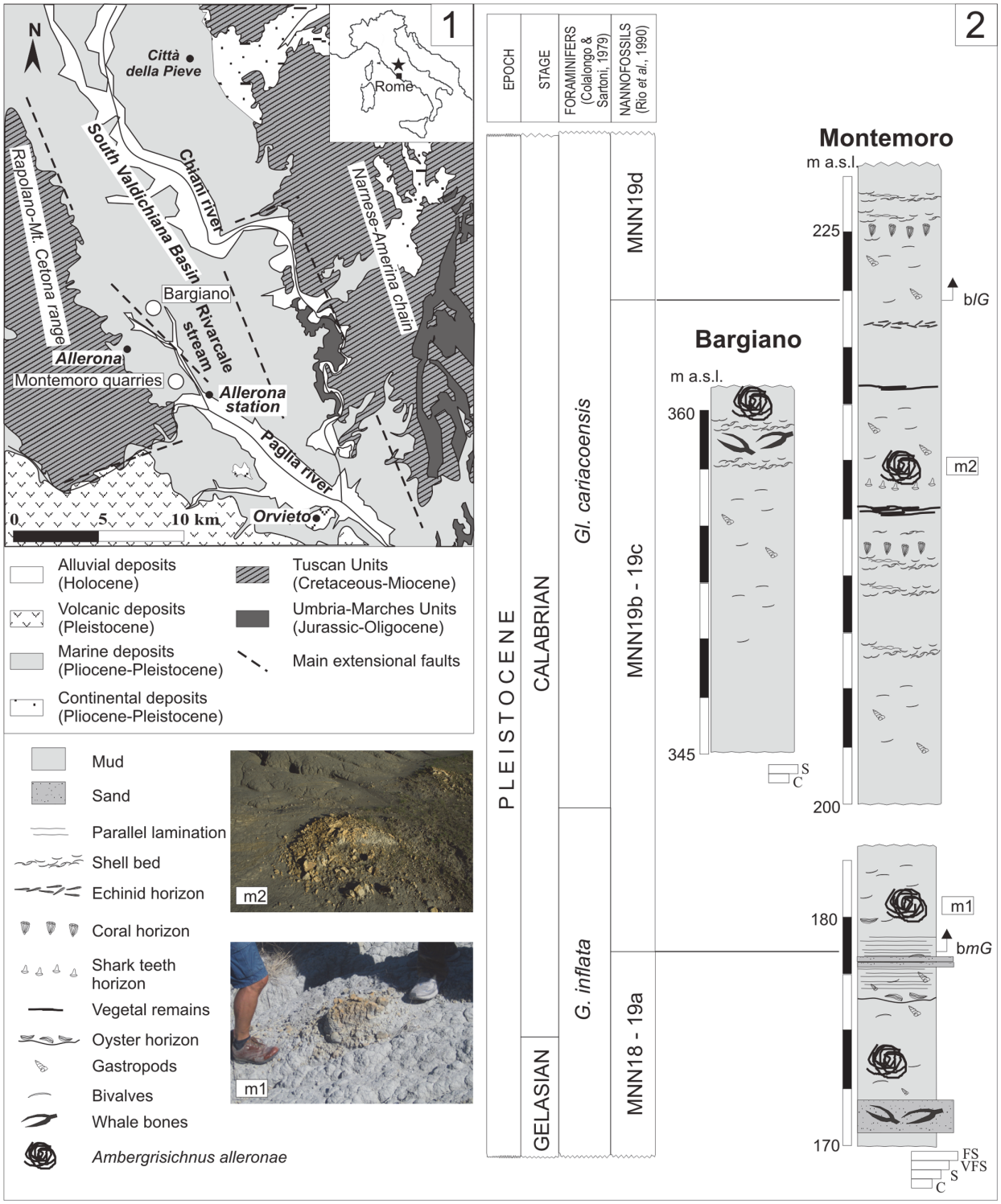

FIGURE 1. 1. Simplified geological scheme for the study area and location of fossil sites (modified after Baldanza et al., 2011). **2.** Bargiano and Montemoro sedimentological and biostratigraphic sections. Pictures (m1, m2) show the emergence of large cololites in the Montemoro section. Grain-size scale: C = Clay, S = Silt, VFS = Very Fine Sand, FS = Fine Sand. *bmG* = base of medium *Gephyrocapsa* event; *blG* = base of large *Gephyrocapsa* event (*sensu* Raffi, 2002).

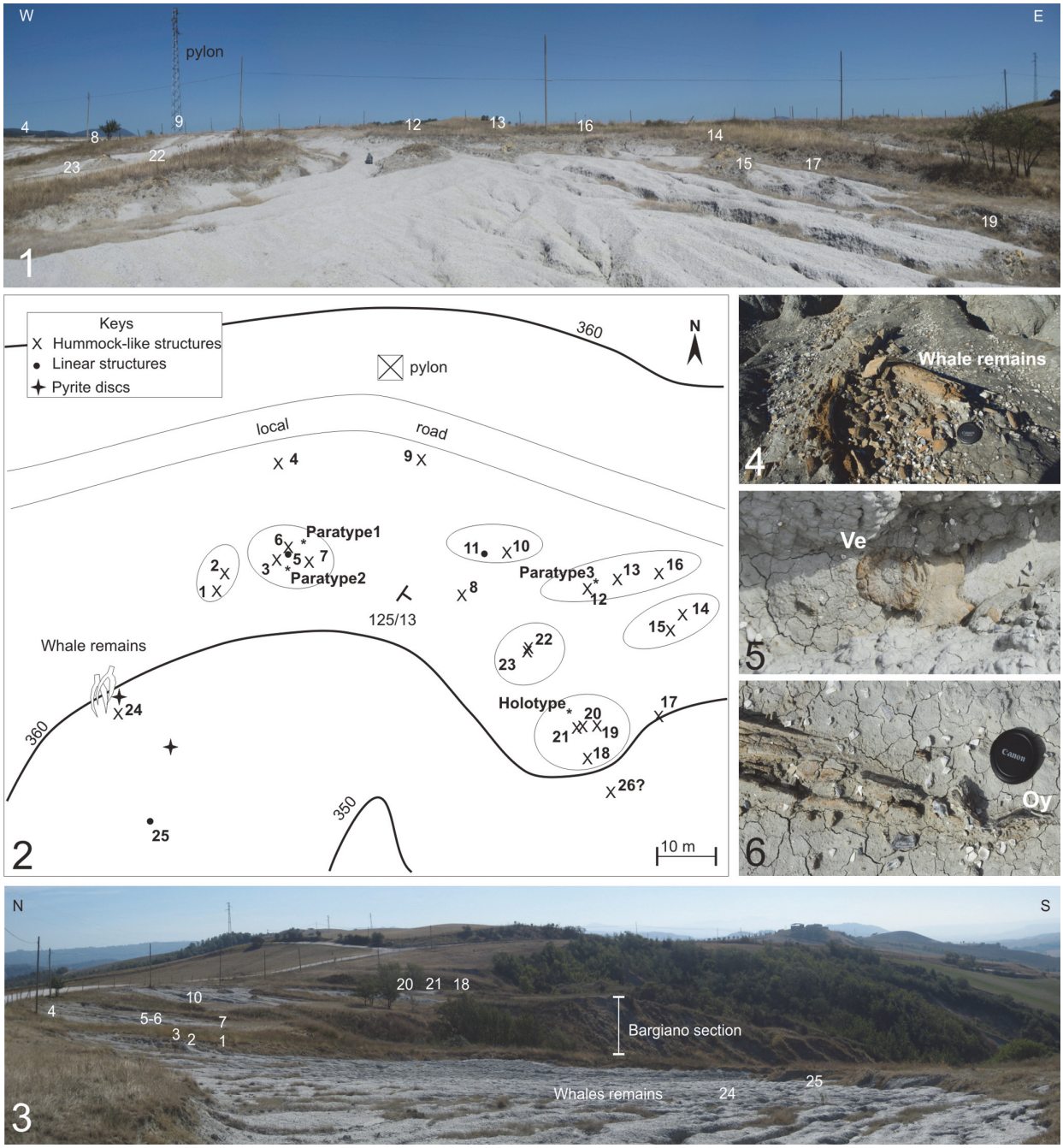

FIGURE 2. Bargiano ichnofossils-bearing site. **1., 3.** Panoramic views of cololites in W-E (**1**) and N-S (**3**) directions. **2.** Simplified topographic map with localization of cololites and whale remains; main bed's attitude is reported. **4-6.** Details of whale bones. **4.** Part of the skull, associated to shell beds. **5.** Cervical fused vertebrae 2nd-7th (Ve). **6.** Oyster shells (Oy) grown on a bone surface.

Montemoro Section

The Montemoro section crops out through a series of quarry fronts, between 170 and 230 m in elevation, on the right side of the Rivarcale stream (Figure 1). Deposits are mainly grayish-blue, massive to thinly laminated silty clay although thin horizons of fine sand occur locally. Beds dip northeastward (020/20). In the lowermost section, the molluscan fauna is rich but oligotypic, and represented by scattered gastropods and bivalve coquinas (Table 1). The uppermost part of the section bears a rich and polytypic molluscan fauna that also includes the chemosynthetic species (CH)

Table 1. Distribution of commonest mollusc, foraminifera and ostracoda species among the study sections. SF = Suspension Feeding; CH = Chemosynthetic species; CA = Carnivorous species; PO = Polychaetes organic compound feedings; IN = Benthic Infaunal; EP = Benthic Epifaunal; Pl = Planktonic; relative abundances: x = rare; X = common; **X** = abundant.

Mollusca	***Affinity***	***Montemoro section (lower)***	***Montemoro section (upper)***	***Bargiano section***	**Foraminifera**	***Affinity***	***Montemoro section***	***Bargiano section***	**Ostracoda**	***Montemoro section***	***Bargiano section***
Dentalium fossile	SF	X	X	X	*Ammonia beccarii*	IN	X		*Acanthocythereis hystrix*		**X**
Dentalium sexangulum	SF	X	X	X	*Ammonia papillosa*	IN	X		*Aurila convexa*	x	
Aequipecten opercolaris	SF			X	*Ammonia parkinsoniana*	IN	X		*Bosquetina carinella*		X
Amusium cristatum	SF	X	**X**	**X**	*Ammonia tepida*	IN	X	x	*Carinovalva testudo*		**X**
Anadara diluvii	SF	X	X	**X**	*Asterigerinata mammilla*	EP	x	x	*Costa edwardsii*	X	**X**
Arctica islandica	SF		x		*Bolivina spathulata*	IN	X		*Cytherella spp.*		**X**
Corbula gibba	SF	x	X	**X**	*Bulimina marginata*	IN	X	X	*Cytherella vulgatella*		X
Glans intermedia	SF		X	X	*Bulimina spinata*	IN	X	X	*Cytheridea neapolitana*	X	X
Glossus humanus	SF		X	**X**	*Cancris auriculus*	EP	**X**	x	*Echinocythereis pustulata*		X
Lucinoma asaphus	CH		X		*Cassidulina laevigata*	IN	X		*Henryhowella ex H. hirta* group	x	
Megaxinus incrassatus	CH		X	**X**	*Gyroidina altiformis*	EP	X		*Krithe praetexta*		X
Myrtea spinifera	CH		**X**	**X**	*Heterolepa floridana.*	EP	x	x	*Pterygocythereis jonesii*	X	**X**
Neopycnodonte cochlear	SF		X	**X**	*Hyalinea balthica*	EP	x		*Ruggeria longecarinata*		**X**
Nucula fragilis	SF		X	**X**	*Lenticulina calcar*	EP	**X**	**X**	*Tyrrenocithere pontica*	x	
Nucula placentina	SF		X	**X**	*Lobatula lobatula*	EP	x				
Ostrea lamellosa	SF		X	**X**	*Marginulina costata*	IN	X	x			
Pecten jacobaeus	SF		X	**X**	*Melonis barleanum*	IN	X	X			
Solemya sp.	CH		X		*Melonis pompilioides*	IN	X	X			
Venus multilamella	SF	**X**	**X**	X	*Nonionella turgida*	IN	x				
Yoldia nitida	CH		X		*Pullenia bulloides*	IN	x				
Aporrhais pespelecani	SF		X		*Quinqueloculina seminula*	EP	x	X			
Epitomium sp.	CA			**X**	*Textularia sagittula*	EP	X				
Euspira catena	CA	X	**X**	X	*Uvigerina mediterranea*	IN	X	X			
Haustator vermicularis	SF	X	**X**	X	*Vaginulina striatissima*	IN		X			
Nassarius italicus	PO	X	X	**X**	*Globigerina bulloides*	Pl	X				
Nassarius clathratus	PO	X	X		*Globigerina cariacoensis*	Pl		x			
Ringicula auriculata	PO	x	**X**	**X**	*Globigerinoides ruber*	Pl	x	X			
Ringicula buccinea	PO		**X**		*Globigerinoides sacculifer*	Pl	x	x			
Turritella spirata	SF	X	**X**	**X**	*Globorotalia inflata*	Pl	**X**				
Turritella tricarinata	SF		**X**	**X**	*Neogloboquadrina* spp.	Pl	X				
					Orbulina universa	Pl	X				

Lucinoma asaphus, *Solemya* sp., and *Yoldia nitida*. Rare specimens of *Arctica islandica* have also been documented. In the lowermost part of the section, an incomplete postcranial skeleton of a mysticeti (presumably a blue whale or a grey whale) and a partially preserved skeleton of a small whale were found some years ago and are still under study (Soprintendenza per i Beni Archeologici dell'Umbria, Pietrafitta Museum, personal commun., 2013). The few, poorly preserved fragments

of small whale were attributed to *Balenula* sp. by Danise and Dominici (2014). The foraminiferal assemblages are characterized by abundant to common benthic infaunal and epifaunal taxa, and by common planktonic species (Table 1). The "cold guest" *Hyalinea balthica* is rarely found. The well-preserved ostracofauna is represented by common carapaces and disarticulated valves (Table 1).

Semiquantitative analysis of calcareous nannofossils reveal, at the base of the section (Figure 1.2), poor assemblages characterized by small *Gephyrocapsa* spp., *Calcidiscus macintyrei,* and *Discoaster* spp., referable to the MNN18-MNN19a Zone (late Gelasian - Calabrian: Rio et al., 1990). Throughout the section, the calcareous nannofossil assemblages increase in abundance, and two biostratigraphic events (b*mG*, base of medium *Gephyrocapsa*, and b*lG*, base of large *Gephyrocapsa*, *sensu* Raffi, 2002) are identified, marking respectively the base of the MNN19b and MNN19d subzones (Figure 1.2) and attributable to the Calabrian (Rio et al., 1990).

Bargiano Section

The 15 m thick section of Bargiano crops out along the rim of badlands, from 350 to 360 m in height, about 100 m higher than the top of the Montemoro section, at the head of the Rivarcale stream (42°50′13″N, 11°58′22″E). It represents the main cololite site (Figure 2). Deposits consist of thinly laminated gray-blue silty clay, with scattered molluscs and coquinas (Figures 1.1-2, 2). Beds slightly dip southeastward (125/13). Mollusc horizons occur throughout the section, and the main shell beds are concentrated around the cololites and close to whale bone remains (Figure 2.4-6). The latter are mainly a few cranial and rib remains, and a small portion of fused cervical vertebrae (probably from 2nd to 7th), attributed to a sperm whale. An oligotypic but rich molluscan fauna is present; the collected species are common species representing a muddy bottom community. Assemblages (Table 1) are largely dominated by epifaunal taxa of suspension feeders, with few infaunal taxa (*Glans intermedia*, *Glossus humanus*, and *Venus multilamella*). Species feeding on polychaeta organic compounds, carnivorous species, and chemosynthetic taxa (indicative of the sulphophilic stage) distinguish the molluscan fauna from Montemoro (Baldanza et al., 2013).

Qualitative analyses of selected samples collected near the cololites and around the whale skeleton were carried out to identify foraminiferal communities. Among the benthic forms, epifaunal taxa are abundant (Table 1). The planktonic foraminifera are rare and represented by *Globigerina cariacoensis*, which identifies the homonymous Foraminiferal Zone (Colalongo and Sartoni, 1979), *Globigerinoides ruber* and uncommon specimens of *Globigerinoides sacculifer*.

The Bargiano ostracod assemblages are quite homogeneous and well preserved, though only disarticulated valves are found. The most abundant species are *Acanthocythereis hystrix*, *Carinovalva testudo*, *Costa edwardsii*, *Pterygocythereis jonesii,* and *Ruggeria longecarinata* as well as many immature specimens of *Cytherella* spp.; *Bosquetina carinella* and *Krithe praetexta* only occur in a few samples, together with *Cytheridea neapolitana*, *Echinocythereis pustulata,* and *Cytherella vulgatella*. The first five species are represented by valves belonging to different stages of maturity and therefore can be considered to a good approximation of an autochthonous community. Regarding their biostratigraphic range, some of these species do not currently live in the Mediterranean, in particular, *Carinovalva testudo* and *Echinocythereis pustulata* are known from Miocene to upper Calabrian and from Zanclean to Sicilian, respectively. *Ruggeria longecarinata* is reported in the Calabrian sediments with *Arctica islandica* of the Monte Mario Formation (Faranda and Gliozzi, 2008).

The calcareous nannofossil assemblages indicate a Calabrian age, because of the occurrence of small- and medium-sized *Gephyrocapsa* spp. (MNN 19b - 19c nannofossil zones: Rio et al., 1990; Raffi, 2002).

MATERIALS AND METHODS

The cololite record is quite different in the two study sections (Figures 1.2, 2.1-3). In the Montemoro section, the presence of cololites (see insert photos m1 and m2 in Figure 1.2) is sporadic and associated with whale bones and shark teeth. At Bargiano, more than 25 large and minor cololites are spread over a surface of 7000 m^2 (Figure 2.1-3). Figure 2.1, 2.3 show how the cololites appeared during September 2011, emerging from the substrate by at least one meter. Locations and mutual distances between cololites are shown in Figure 2.2. This study focuses only on the Bargiano cololites, due to the poor preservation of cololites at Montemoro. The description of *Ambergrisichnus alleronae* igen. et isp. nov. is based on four selected samples (labelled respectively CT01, CT02, CT03, and CT04), which are considered the most representative. Fragments from five large cololites (labelled 8, 9, 12, 15, and 17 in Figure 2.2)

were used for thin sections, mineralogical analyses and scanning electron microscopy (SEM). Several pyrite disks of about 0.5-2.0 cm in diameter, scattered through the clay sediments near whale bones and cololites, were collected and studied with a scanning electron microscope (SEM) to provide a preliminary analysis of the microstructure (Figure 2.2). Qualitative mineralogical compositions of the analysed samples were performed by X-ray powder-diffraction (XRPD) by means of an automatic diffractometer (Philips PW 1830/1710) in the following experimental conditions: Bragg-Brentano geometry, Ni-filtered CuK_{α} radiation obtained at 40 kV and 20 mA, 5-60° 2Θ investigated range, 0.02° step, 2 s counting time per step. The total amounts of volatile compounds were determined by thermogravimetry analysis (TG) by means of TG-DSC equipment (TA Instruments, model Netzsch STA 449C *Jupiter*). The experimental conditions were: (a) continuous heating from room temperature (20 °C) to 1000 °C at a heating rate of 10 °C min^{-1}; (b) inert-gas (N_2) dynamic atmosphere (30 ml min^{-1}); (c) alumina, top-opened crucible; and (d) no thermal pre-treatment of the samples, to prevent a possible mass loss of weakly bonded H_2O molecules.

RESULTS

Among the cololites, two morphotypes are distinguished, indicated herein as relatively simple and complex cololites, respectively. The “simple” cololites are found as isolated, relatively smaller specimens (Figure 3.1-7), and/or as disarticulated portions of complex structures (Figure 4.4). They are elongate, 30–40 cm wide, exceptionally up to 60 cm, and rarely branched. Smaller simple cololites are 20 to 25 cm wide and 18 to 35 cm long (Samples CT01, CT02; Figure 3.1, 3.3). Characteristically, an internal concentric structure is visible (Figure 3.4-6), exhibiting concentric bands, a few mm thick, and bulges (Figure 3.2). The latter, which are oval to round positive compressed structures (exceptionally up to 12 cm, but commonly 5-6 cm wide), correspond to the *rognons* described by Clarke (2006) in Recent ambergris. Bulges are irregularly dispersed on the outer parts of simple cololites (Figure 3.2), but may be also observed within complex cololites as fragmented parts. In longitudinal view, the outer surface of simpler cololites often shows a longitudinal set of striae (Figure 3.1, 3.3, 3.5, 3.7). Two kinds of striae are identifiable. The first are small and irregular, weakly prominent, and disposed on the outer surface of rings (Figure 3.5); the second type, are 1–3 cm wide and up to 12 cm long, are deeply striate (Figure 3.1, 3.3, 3.7) and converge towards an apex, whose tip tends to be tapered (Figure 3.3). Tapering and deep striae, therefore, are the most typical features of the simpler cololites and commonly occur in many specimens (up to 70% of total). Rare oblique, larger but shallower striae have been found on some outer surfaces. Other types of deformation, such as mammellons and ridges, are disposed along the outer surfaces with abrupt change in colour (e.g., from yellowish to red, Figure 3.4).

The complex cololites (Figure 4.1-4) are hummocky structures, varying in shape and dimensions (30–60 cm high and 60–120 cm wide), and protruding from the surrounding clay deposits to produce conical mounds (Figure 4.1-4). Less frequently, they are almost straight cylindrical structures (Figure 4.5-6). Typically, a single easily recognized structure is 50 cm high and 80 cm wide and shows a concave, irregular center and a subcircular to elliptical outline (Figure 4.1, 4.3). A complex structure consists of a tangle of rough or concentric tunnels, from 20 to 40 cm in diameter, or, more rarely, of an accumulation of irregular slabs (Figure 4.4). Typical convergent striae, described in simpler cololites, are located at the end of peripheral tunnels. The outer parts of tunnels are commonly rotated and show varied configurations (Figure 4.1-2). Convolution occurs principally in the center of complex structures. Colors vary from ochre (yellowish or red) to whitish or light gray, commonly with color gradations (e.g., red) in the same structure. The complex cololites are made of several close, juxtaposed simpler structures, without crystalline cements; thus the cololites easily undergo mechanical disarticulation and disaggregation (Figure 4.4). The holotype for *Ambergrisichnus alleronae* has been selected from one of the better-preserved simpler structures (Sample CT01, Figure 3.3 lateral view). The specimens CT02, CT03, and CT04 are designed as paratypes (Figure 3.1-2, 3.5-7).

SYSTEMATIC ICHNOLOGY

Ambergrisichnus alleronae igen. et isp. nov.
Figure 3.1-7

zoobank.org/862C00F-14BE-490E-9628-6115E88A7CFC

zoobank.org/5ECB7CBB-3D47-4EA7-8374-D5D2CCB2FF2B

Etymology. From the term *ambergris* (originally from Arabic *ambar*), indicating a solid substance usually associated with sperm whales (*Physeter macrocephalus* Linnaeus, 1758) and less commonly with pygmy sperm whales. The species

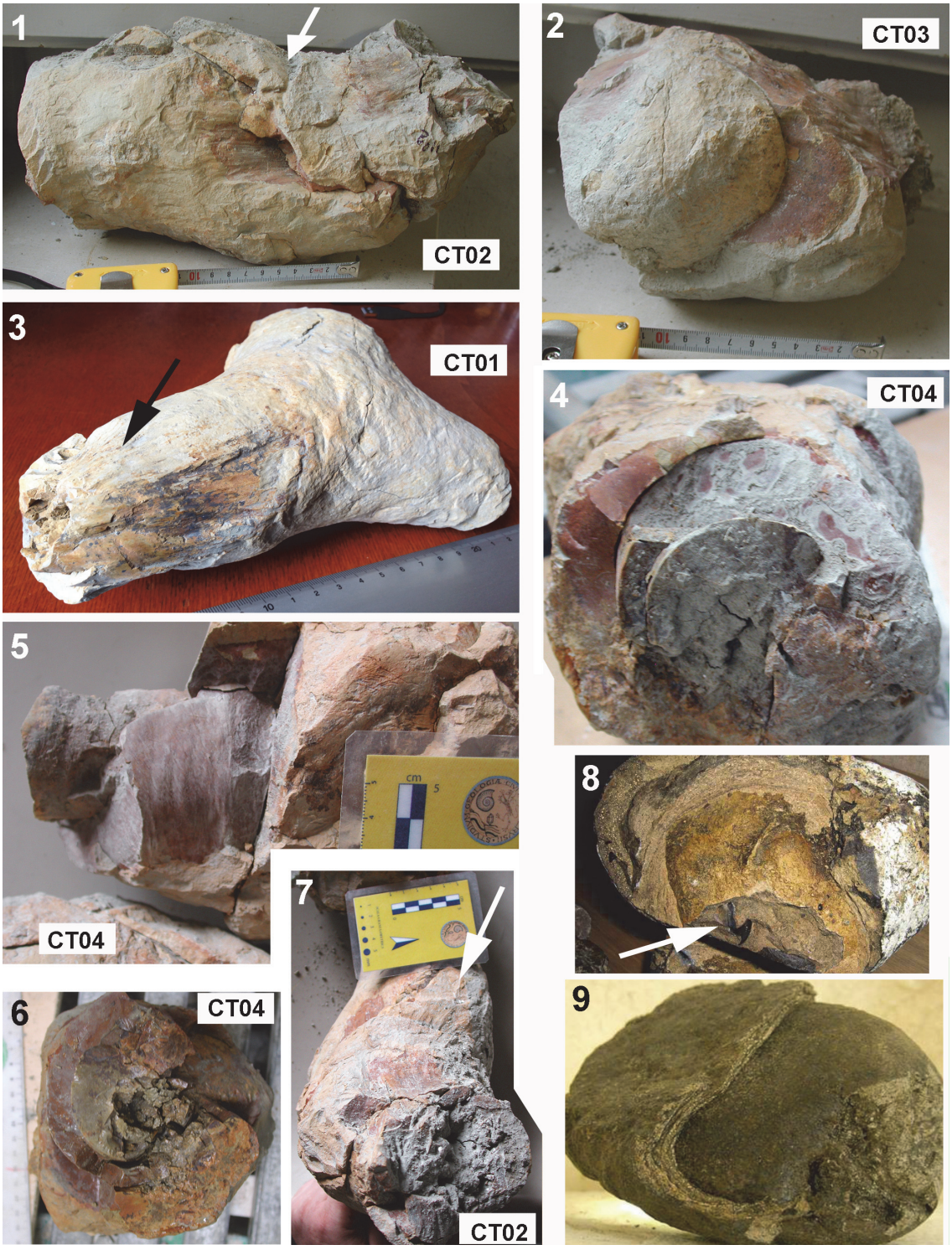

FIGURE 3. Simpler cololites (intestinelite group) from Bargiano section. **1., 7.** Typical irregular elongated mass (CT02), produced by different helicoidal swirls, Bargiano section, in lateral view (**1**) and backside view (**7**). Arrows indicate the occurrence of longitudinal striae. **2.** Mass (CT03) with bulges (rognons). **3.** Holotype of *Ambergrisichnus alleronae* (CT01), showing converging striae in the left apex (arrow) and enlargement at the other apex. **4.** Characteristic helicoidal arrangement and rings with different colours (CT04). **5-6.** Side view (**5**) and front view (**6**) of rings (CT04), (modified after Baldanza et al., 2013). **8-9.** Modern examples of ambergris masses with concentric rings and changes in colour, comparable to study specimens (arrow in 8 indicates a squid beak).

FIGURE 4. Complex cololites (intestinelite group), Bargiano section. **1., 4.** Hummock-like cololite (n 8 in Figure 2.2), 50 cm high and 80 cm wide, with a concave, irregular center and outer sub-circular to elliptical tunnels (**1**). Disaggregated portions (**4**) reveal both striae and concentric structure. **2.** Hummock-like cololite (n 12 in Figure 2.2) formed by an accumulation of irregular, elongated slabs. **3.** Complex hummock-like structure (n 15 in Figure 2.2) with irregular, meandering tunnels disposed at various levels. **5.** Isolated linear cololite (n 25 in Figure 2.2), 20 cm in diameter, partially emerging from clay deposits. **6.** Irregular, 60 cm long linear cololite (n 11 in Figure 2.2), showing spiral coiling at the right side.

refers to the name of the village of Allerona, near Orvieto, in western Umbria, central Italy, were it was first found.

Material. Four specimens (one holotype and three paratypes).

Holotype. Specimen CT01 (Figure 3.3), (length 18 cm, width 20 cm), housed in Biosed Lab, Department of Physics and Geology, University of Perugia.

Paratypes. Specimens CT02 (Figure 3.1, 3.7), CT03 (Figure 3.2), and CT04 (Figure 3.5-6), housed in Biosed Lab, Department of Physics and Geology, University of Perugia.

Type locality. Bargiano badlands, 2 km northeast from Allerona, in southwestern Umbria, 42°50′13″N, 11°58′22″E, in offshore marine clay deposits of the Chiani-Tevere sedimentary cycle, Chiani-Tevere unit.

Stratigraphic range. Early Pleistocene, Gelasian to Calabrian, about 1.95-1.55 Ma (Baldanza et al., 2011; 2013)

Diagnosis. Ichnogenus: irregularly cylindrical permineralized structure, elongated or branched (Figure 3.3), with apex showing convergent striae and strong tapering towards the tip. Dimensions varying from 20 to 40 cm (exceptionally up to 60 cm) in width, from 18 to 35 cm in length. Smooth or slightly rough outer surface (Figure 3.1, 3.2, 3.7) showing compressional structures and irregular striae, with interposed oval to subspherical and/or compressed bulges (up to 7 cm wide and 9 cm long), emerging abruptly from the surface. Concentric helicoidally envelopment in cross section, converging towards a poorly cemented nucleus (Figure 3.4, 3.6), with colour changes and locally exhibiting thin concentric bands.

Ichnospecies: as for the ichnogenus.

Description. The holotype of *Ambergrisichnus alleronae* isp. nov. (CT01, Figure 3.3) is an irregular cylinder, 18 cm long and 20 cm wide, with one apex showing convergent striae and strong tapering toward the tip, while the other apex is wider and includes two very short branches (Figure 3.3). In cross section, the concentric envelopment, best visible on paratype 3 (CT04), converges towards a nucleus that is poorly cemented (a marly clay, Figure 3.4, 3.6). The external texture is smooth or slightly rough. In paratype 3, one apex has been cut to show the interior arrangement of rings and the helicoids; the helicoids, 10 to 40 cm thick, are well preserved, with colour changes and locally exhibit concentric bands. The outer surface of paratypes 1 and 2 (Figure 3.1, 3.2, 3.7) show compressional structures and irregular striae, and between these structures there are some *rognons* (bulges: Clarke, 2006). The *rognons*, emerging abruptly from the outer surface, are oval to subspherical; they are up to 7 cm wide and 9 cm long, and compressed. The major change in colour is between striae and *rognons*, and similar features occur in modern and ancient cololites (Hunt and Lucas, 2012a). The holotype represents the tip of a complex cololite hummock. About 30% of the terminal parts of outer sheaths of complex cololites exhibit comparable characteristics, although the shape can change (e.g., no branching). Morphological features of the holotype and the paratypes of *A. alleronae* igen. et isp. nov., such as striae, concentric bands, and *rognons* are recognized in many large masses (e.g., complex cololites), as well as in modern ambergris (Clarke, 2006).

Remarks. The Allerona specimens differ from other similar large structures induced by diagenetic processes, because of the external shape and internal structures both of complex and simpler cololites. Although externally it may resemble vertebrate and invertebrate burrows (Gaillard et al., 2013, Figures 6 and 8), or shafts of *Tisoa siphonalis* from the Early Jurassic (Pliensbachian) (van de Schootbrugge et al., 2010), *A. alleronae* differs significantly in important aspects. The internal arrangement of *A. alleronae* is helicoidal or concentric around a central nucleus (usually a dark grey clay core, Figure 3.6); this feature is lacking in most invertebrate burrows, as well as in the simple or columnar, abiotic carbonate concretion of *Tisoa siphonalis*. Moreover, a well-cemented series of concentric bands (Figure 3.4-6), generally with oxidized reddish or yellowish crusts, is common in the specimens of *A. alleronae* (Baldanza et al., 2013, Figures 3.1 and 3.2), and are very similar to those present in modern ambergris (Figure 3.8-9). In the holotype (Figure 3.3) the external branched shape resembles some giant *Thalassinoides* in the Early Jurassic Calcari Grigi Formation of the Southern Alps (Giannetti and Monaco, 2004), but in the latter specimens convergent striae and concentric rings are absent. In cross section, large *Thalassinoides* (type 4 of Giannetti and Monaco, 2004) shows a central large tunnel used by the crustacean for movements within the burrow. This feature is lacking in *A. alleronae*. The converging striae of *A. alleronae* are typical and never found in other fossil marine or freshwater cololites, although spiral bromalites are known and have been associated with primitive fish, for example freshwater sharks *Orthacanthus* (Shelton, 2013). Striae are reported in other trace fossils such as the aestivation burrows

of lungfish from the Eocene to Oligocene of south-eastern France (Gaillard et al., 2013). Nevertheless, these striae are short and parallel, of the same width and regularly spaced, while striae of *A. alleronae* are convergent towards the apex and of irregular length (Figure 3.3).

Discussion. The holotype of *A. alleronae* (CT01) is a portion of a large cololite formed as hummocks with many convolute tunnels, which has never been found in branched horizontal mazes of *Thalassinoides* (Monaco, 2000; Monaco et al., 2007). Notably, the orientation of ambergris specimens, which is known only in two finds from the *Southern Harvester* floating factory obtained during the Antarctic whaling season of December 1953 (155 kg and 421 kg specimens), has the smaller end pointing towards the anus and the larger end pointing towards the stomach of the whale (Clarke, 1954, 2006). Similarly, the end of each Allerona structure is tapered and exhibits wide and deep convergent striae, as in ambergris described by Clarke (2006). Subcircular lumps and protruding structures are common in the outer part of *A. alleronae*, just as in the *rognons* found in present-day ambergris (Clarke, 1954, 2006, figure 4; Johnson, 2001; Perrin, 2005; Vogt, 2011). Clarke (2006) observed that the thinner end of each mass of ambergris may be tapered, or shaped like a thick bobbin protruding from the main mass, with a somewhat rounded terminus. The passive movement of the ambergris mass in the intestinal tract can produce such structures as large striae and compression of rognons as described in modern ambergris masses (Clarke, 2006). Comparable features had not been reported in the paleontological and ichnological records, until the work of Baldanza et al. (2013). The findings of squid beaks within cololites (Figure 5.1-4) further support the connection with Recent ambergris masses, wherein squid beaks are conspicuous.

Mineralogical Analyses

Baldanza et al. (2013) reported preliminary mineralogical data by FTIR analyses performed on the inner gray and outer red or yellow parts of cololites. The FTIR analysis showed a relatively low amount of aluminum silicates within the fossil structures, while the enclosing clay sediments showed a low content of $CaCO_3$ (<15%); the $CaCO_3$ in the cololites was interpreted as biogenecally precipitated due to local enrichment in organic matter (Castanier et al., 1999; Douglas, 2005). X-ray diffraction spectra of the new analysed samples are presented in Figure 6.1. XRPD analysis shows that samples are essentially made up of dolomite, with minor amounts of quartz and phyllosilicates, and traces of calcite and plagioclases. Thermogravimetric analysis (Figure 6.2) confirms the presence of volatile compounds related to the carbonate phases. Assuming that all the mass loss in the temperature range of 600-1000 °C may be attributed to carbon dioxide bound to dolomite, the amount of this carbonate phase ranges from 72% (sample 15) to 81% (sample 17) in weight.

A preliminary observation under the scanning electron microscope of the inner portions of cololites allowed us to identify a microcrystalline mosaic of rosette-shaped dolomite with mica (probably muscovite) crystals in the inner portion (Figure 7.9), and scattered dolomite nanocrystals associated with spheres of probable bacterial origin (Figure 7.10).

Microstructural Arrangement

The analysis in thin sections of different cololites has highlighted the pervasive presence of a micropeloidal matrix with microcrystals of dolomite, pyrite crystals, scattered benthic foraminifera, and other, and never observed peculiar structures. The micropeloids (Figure 7.4-7) are very small, on an order of few microns, and might be the result of the original degraded microbial mat as indicated by Chafetz (1986). The distribution of pyrite crystals varies through the cololite bodies; the peripheral region of *Ambergrisichnus alleronae* (generally red or yellow-orange in colour) shows a much higher pyrite concentration (as small grains of 30-40 μm) than the interior region, where the pyrite formed framboids. The framboidal, from 50 to 100 μm, pyrite crystals (Figure 7.3, 7.6, 7.8) occur as isolated or grouped (Figure 7.8), and pyrite also infill microfossils (benthic foraminifera *Bulimina* and *Bolivina*) (Figure 7.5-6).

A large number of dolomite crystals of different size (Figure 7.4-6, 7.8) is scattered in the matrix and in some cases, the micrometric crystals constitute the matrix of cololites (Figure 7.6). Other particular types of structures, such as long chains of pyrite spherules (Figure 7.1, 7.3) and elliptical bodies with central pyrite crystals (Figure 7.4), are identifiable into cololites and could be comparable with structures produced by filamentous large sulphur bacteria like *Beggiatoa* and *Thioploca*. *Beggiatoa* (Figure 7.2, free-living specimens) is a candidate for a source because of its morphology, represented as a single free-living filament with sulfur inclusions (Salman et al., 2011). Other discoid pyritized structures (ranging in diameter from

FIGURE 5. Squid beaks from structure n 8 (Figure 2.2). Part of a lower beak (**1**) and longitudinal section of a beak (**2**), emerging from the rough surface of rock sample. **3-4.** Microscopic features of squid beaks inside cololites (structure n 12, Figure 2.2). Crystals and framboids of pyrite (**4**), scattered into the micropeloidal matrix with dolomite microcrystals are also visible (**1** and **4** are modified after Baldanza et al., 2013).

0.5 to 2.0 cm), were commonly found close to the cololites and near the whale skeletal remains (Figure 7.11-13). Several discs are circular, with a rough surface, undulate margins, and an umbonate to convex central area. From a microbiological point of view, they are comparable to colonies or structured communities of bacteria (Branda et al., 2001; Kearns et al., 2005; Granek and Magwene, 2010). Observation under the scanning electron microscope, indeed, revealed a rough surface formed by microspheres of pyrite, attributable to original bacterial bodies. The only known comparable structures are the “discs of pyrite in coal” described by Southam et al. (2001) as an example of fossilized bacterial colonies.

DISCUSSION

Ichnological Significance

Undoubtedly, the described permineralized structures appear to be cololites of marine mammals, and specifically of sperm whales. But what kind of cololites? Two main groups are recognized: intestinelites (preserved within a body cavity) and evisceralites (preserved outside a carcass) (Hunt and Lucas, 2012a). Bromalites are considered remains of material sourced from the digestive system of organisms and, in the majority of cases, deposited externally (Hunt et al., 2012), as, for example, the well-known types of fossilized spiral faeces. Regurgitalites (from oral cavity), evisceralites, and coprolites are thus known only after they leave the body of the producing organisms, whereas gastrolites (stomach contents) and intestinelites are found *in situ* in their respective organs (Hunt et al., 2012). The internal and external structures of all these groups can change, following characteristics of organisms and environments. An emblematic case is represented by spiral coprolites (Shelton, 2013); many authors debated whether or not these spiral structures were preserved after being expelled as faeces, or if they were retained

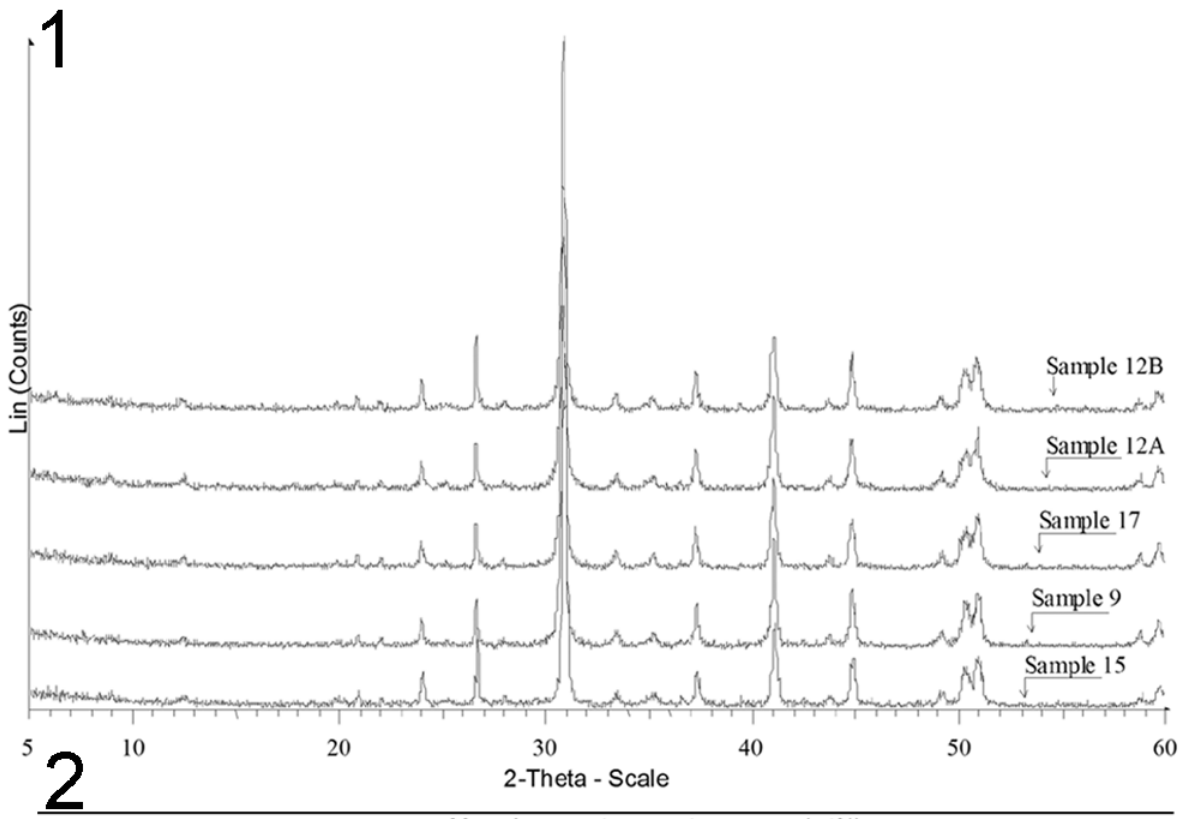

	Mass loss per temperature range (wt%)									
Sample	<120	120-200	200-300	300-400	400-500	500-600	600-700	700-800	800-900	900-1000
15	0.70	0.24	0.24	0.30	0.42	1.65	4.82	19.99	9.28	0.05
9	0.42	0.19	0.24	0.32	0.60	2.01	7.57	25.01	5.60	0.08
17	0.43	0.08	0.04	0.09	0.31	1.23	5.18	20.82	12.42	0.05
12A	0.48	0.14	0.12	0.22	0.44	1.45	5.85	25.66	6.70	0.08
12B	0.57	0.10	0.04	0.12	0.50	1.24	4.61	24.10	6.58	0.04

FIGURE 6. XRPD patterns (**1**) and mass changes in thermogravimetric analysis (**2**) of five cololite samples. Numbers of samples correspond to the structure of provenance (Figure 2.2).

after death in the colon or rectum of the animal (Williams, 1972; Stewart, 1978; Duffin, 1979; Mcallister, 1985; Shelton, 2013). The coprolites described at Allerona undoubtedly differ from any other known bromalite in the occurrence of internal spirae, often forming thin concentric bands. They also differ considerably in length and other dimensions, occurrence of branches, long tunnels, and meanders. Cololites, in the case of large marine mammals, can form irregular masses with many, often meandering tunnels that follow the original contours of the gastrointestinal tract (e.g., stomach, colon, rectum), producing striae and tapering close the rectum and elongated bulges as rognons. Therefore, *A. alleronae* is ascribable to the cololite group and could be referred to as an intestinelite, which are intestinal contents within the body, or to evisceralite if they are found in the absence of a carcass, using the terminology of Hunt et al. (2012a). Thus, *A. alleronae* igen. et isp. nov. clearly represents an evisceralite since they are found without a skeleton or carcass.

Diagenesis and Preservation of Fossil Ambergris Masses

The preliminary chemical data reported by Baldanza et al. (2013) reveal the presence of organic molecules compatible with the degradation of cellular lipids and with the mammalian gastric (or intestinal) activity. The discovery of eight free amino acids shows a close correlation with the composition of squid beaks. The occurrence of many permineralized squid beaks (Figure 5) and

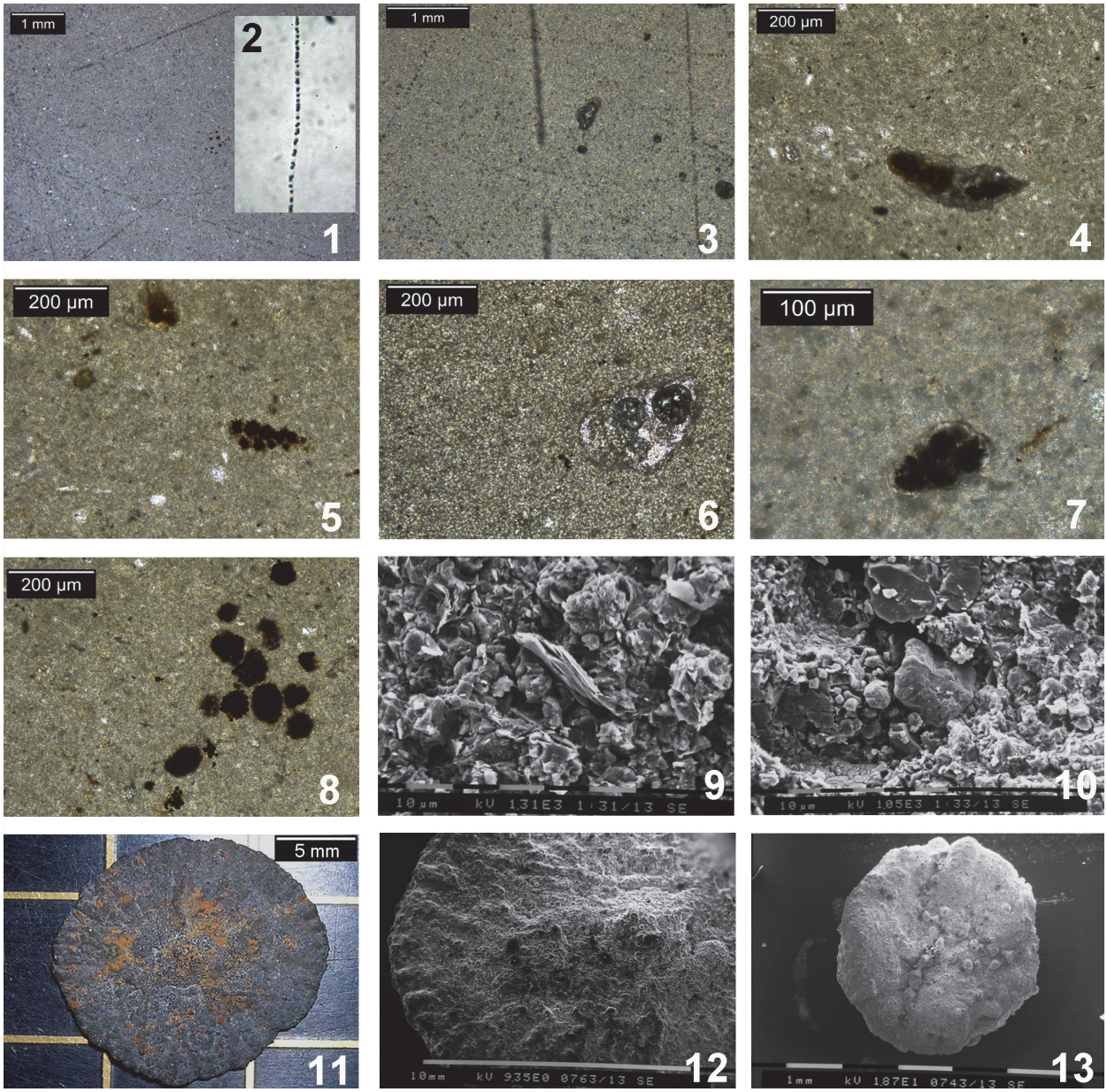

FIGURE 7. 1, 3-8. Transmitted light photomicrographs of petrographic thin sections of the Bargiano cololites. **1.** Interior of cololite (structure n 12) showing a micropeloidal matrix crossed by long chains of pyrite microgranules. **2.** *Beggiatoa* specimens, sulphur large bacteria, single free-living filament with sulphur inclusion. **3.** Detail of fossil *Beggiatoa*-like filaments from structure n 12. **4.** Subspherical, red-brownish micromasses of pyrite (or sulphur), surrounded by a grey "halo" that inglobates all. To note the micropeloidal matrix. This structure may be comparable with large *Thioploca* cells. **5-7.** Benthic foraminifera, partially and/or totally filled by bacteria-induced microcrystals of pyrite. **8.** Pyrite framboids from structure n. 12. **9-10.** SEM images of cololite internal fragments.The both surfaces are fresh, no acid attack was made. **9.** Rosette structures made of dolomite microcrystals, and scattered single spherical cells referable to bacteria. In the centre, mica crystals with typical shape. **10.** Dolomite crystals with well-developed orthorhombic shape (at central right), sparse spherical cells of bacteria, and a quartz crystal. Dolomite crystals (left) are aggregated to form a compact mass. **11-13.** Bacteria-induced pyritization (sun-like pyrite discs). **11.** Stereomicrophotograph of a large pyrite disc (about 1.5 cm in diameter). **12.** SEM image of disc surface (particular), showing a large amount of spherical cells, progressively smaller form center to periphery. This arrangement is associated to bacteria colonies. **13.** Small pyrite disc, yellow/orange, with elliptical to dumb bell shaped bacteria bodies arranged in a short chain.

altered organic matter confirm the origin of *A. alleronae* as being related to sperm whales.

The original mineralogical results proposed herein open new problems involving the permineralization processes of sperm whale cololites, accumulating within the intestine as masses of ambergris, and rich in organic substances (ambrein, intestinal parasites, squid beaks, etc.). The first chemical investigation of fresh ambergris masses (Baynes-Cope, 1962), involved the spectrographic analysis of ashes, obtained by ignition below 500 °C, revealed the perennial occurrence of magnesium and calcium (potential sources for a dolomite formation), with small amounts of sodium, manganese, iron, and silicon. The extensive occurrence of nano- and microcrystals of dolomite in our samples leads us to consider the microbial mediation as a possible mechanism for natural dolomite formation at low temperatures (Vasconcelos et al., 1995; Van Lith et al., 2003). In particular, the dolomite nucleated exclusively in bacterial colonies, intimately associated with extracellular organic matter and bacterial cells (Gram-negative bacteria) and laboratory research demonstrated the specific adsorption of Ca^{2+} and Mg^{2+} onto cell surfaces, indicating the role of bacterial films in carbonate nucleation and bacterial fossilization (Van Lith et al., 2003). Experimental data has demonstrated that microbial sulphate reduction can be responsible for the formation of carbonates with different Mg/Ca ratios (Sagemann et al., 1999; Warthmann et al., 2000). In addition, the bacterial sulphate reduction may overcome the kinetic barrier to dolomite formation by increasing pH and carbonate alkalinity, and as a consequence, sulphate occurs in sea water as a magnesium sulphate ion pair, while removal of sulphate ions by bacteria may increase the availability of magnesium ions for dolomite precipitation (Vasconcelos et al., 1995; Vasconcelos and McKenzie, 1997; Castanier et al., 1999; Wright, 1999; Warthmann et al., 2000). All these processes can easily justify the extensive occurrence of dolomite in our samples. Other evidence supporting the microbial-induced mineralization, linked to the presence of bacteria within the cololites, includes the occurrence of bacterial chains visible in thin sections, and the common presence of pyrite framboids and micropeloids (Figure 7). Heterotrophic bacteria are presumed to diffuse and develop into the ambergris masses, feasting on the rich lipids; as shown by Nagakuma et al. (1996), the presence of fatty acids stimulates the presence of methane-oxidizers in association with sulphate-reducers, analogous to the ecosystem that occurs around methane seeps (Orphan et al., 2004). Thus, it might be reasonable to suppose that heterotrophic bacteria, buried into ambergris masses, degrade organic compounds producing sulphide that can be converted to pyrite (Allison et al., 1991; Hurtgen et al., 1999; Shapiro and Spangler, 2009). This process is related to the sulfophilic stage, the last of the three stages described by Smith and Baco (2003) for whale-falls, in which elevated H_2S concentrations within whale bones and surrounding sediments lead to sulphite-based chemoautotrophic primary production. The excess of sulphur from sulphur-bearing amino acids or other organic sulphur compounds in the tissue (in our case the ambergris masses, enriched in free amino acids derived from squid beaks) reacts as H_2S with iron monosulfide to produce pyrite. Moreover, as demonstrated by Zopfi et al. (2008) the *Thioploca*/*Beggiatoa* community couples the biogeochemical cycles of nitrogen and sulphur. Our approach is currently based on morphological comparison, and will require specific analyses aimed at identifying traces of bacterial biomarkers. In the absence of geological evidence for a cold seep, the marine sea floor of Bargiano, enriched by the accumulation of multiple sperm whale carcasses, probably simulated a paleoenvironment enriched in methane, originating from the processes of degradation of organic tissues. This particular situation altered the water chemistry, stimulating the proliferation of bacterial mats, and created suitable conditions for the precipitation of biogenic dolomite and the development of iron sulphides.

Palaeoenvironmental Implications

Based on sedimentological and micropalaeontological data, the study sections are referred to offshore marine environments (Baldanza et al., 2011, 2013). The occurrence of horizons bearing plant remains throughout the sections, the grain size of the sediments, and the foraminiferal assemblages lead us to hypothesize a distal source of sediments from emergent areas nearby (Baldanza et al., 2011, 2013). Thus, average water depths must have been between 100 and 150 m, as confirmed by analyses of the ostracod fauna. *Acanthocythereis hystrix* is documented today in the Gulf of Noto at -70 m, and in the Gulf of Taranto between -57 and -107 m (Bonaduce and Pugliese, 1979; Montenegro et al., 1998). *Costa edwardsii* is reported in the Gulf of Naples between -42 and -92 m depth, and in the Adriatic Sea between -24 and -125 m. Finally, *Pterygocythereis jonesii* is noted in the Adriatic Sea between -80 and -170 m and off

Malta between -9 and -128 m. *P. jonesii*, though considered as ubiquitous, is also present at depths greater than those of the upper circalittoral zone; *Henryhowella* is likewise considered as a ubiquitous genus and is reported from infralittoral to bathyal zones (Guernet and Lethiers, 1989). Hence, based on the available data it is possible to utilize the ostracod association to indicate a depositional palaeoenvironment located on the continental shelf between the upper circalittoral and middle circalittoral zones (50-150 m water depth). It should be noted that the association contains no specimens that could be considered as allochthonous or definitely transported from shallow coastal environments. The infaunal taxon *Krithe* digs into the sediment to eat bacteria and microbes. The abundance of some species such as *Pterygocythereis jonesii* and *Acanthocythereis hystrix* is particularly interesting. This abundance could have been created, in all probability, by an increase of nutrients in the bottom. An increase in abundance of some species of ostracods in relation to the increase in trophic resources is a phenomenon that has been reported by several authors, among others Coles et al. (1996) in the Porcupine Basin, Sciuto (2005) in the Pleistocene sediments of Capo Milazzo, and Di Geronimo et al. (2005) in the Pleistocene of Furnari.

The malacofauna, which is described throughout the sections, is not particularly diagnostic bathymetrically, and it could be generically referred to the circalittoral zone. According to Murray (2006), some information about the palaeoenvironmental conditions at the seafloor can be extrapolated from the ecological characteristics of benthic foraminifera.

The dominance of epifaunal and shallow infaunal foraminifera taxa confirms an adequate availability of nutrients in the form of degraded organic matter. Epifaunal and infaunal taxa indicative of cool conditions (Murray, 2006) at the sea floor (*Hyalinea balthica*, *Lenticulina calcar*, *Heterolepa floridana*, *Gyroidina altiformis*, and *Melonis* spp.) are present. Contrary to the Bargiano section, where cool conditions are confined to the seafloor, in the Montemoro section planktonic foraminifera assemblages indicate almost constant cool conditions throughout the water column.

Biostratinomic and Taphonomic Inferences

The occurrence of *A. alleronae* through the Montemoro and Bargiano sections is documented in at least four distinct horizons. The nannofossil events recognized in the Montemoro section allow the estimate of a sedimentation rate between 182 and 113 mm ka^{-1}. According to previous data (Baldanza et al., 2011, 2013), sedimentation rates for Pleistocene marine clay deposits in the study area are between 75 and 102 mm ka^{-1}: thus, the 1 m-thick clay bed with *Ambergrisichnus alleronae* at Bargiano could have been deposited in about 10 ka. Throughout the Montemoro section, the main trace fossil events are dated about 1.80, 1.75, and 1.65 Ma, with intervals of 50 ka and 100 ka between successive events, respectively. The larger cololites at Bargiano can be grouped in seven main groups, with five other isolated objects (Figure 2.2). Including the whale skeleton, 7 to 13 sperm whales were presumably present at the site inside the same 1 m-thick clay bed and spread over a surface of about 7000 m^2. As first pointed out by Baldanza et al. (2013), this concentration is indubitably high, and hypotheses are needed to explain these numbers. Because of the presumed depth, this record is more compatible with whale-fall events than to stranding events. In reconstructing a possible scenario, significant evidence is provided by the fact that molluscs characteristic of whale-fall communities were found by the whale bones and cololites alike. The mollusc assemblage peculiarities reveal some important similarities with whale-fall communities (Dominici et al., 2009; Danise et al., 2010; Baldanza et al., 2013). The presence of chemosynthetic bivalves (*Megaxinus incrassatus* and *Myrtea spinifera*) and of gastropods that eat the polychaetes organic compounds (*Nassarius italicus* and *Ringicula auriculata*), evinces a large availability of nutrients and organic matter at the seafloor. This hypothesis is consistent with the abundance of filter feeders and suspension feeders. The presence of whale-fall mollusc assemblages in this context is suggestive of one or more distinct mass mortalities of sperm whales. The carcasses that originally accumulated on the seafloor are not preserved. The presence of more than 25 cololites of variable size and shape may be the only record of this mass mortality, the causes of which are not yet identified. The lack of cetacean remains around the structures (with the exception of one case) can probably be ascribed to several processes that have contributed to destruction of whale carcasses as in modern whale falls in the Pacific and Atlantic Oceans (Smith and Baco, 2003). According to Smith et al. (2002), the ecological succession of scavengers and other opportunistic taxa proceeds more quickly at shallow depths than in deep sea whale falls. Some foraminifera that consume large amounts of bacteria (Mur-

ray, 2006), such as *Ammonia* spp., *Textularia* spp., *Bolivina spathulata*, *Bulimina marginata*, *Bulimina spinata,* and *Cassidulina carinata*, argue for bacterial mat growth on the seafloor. Thus, the flux of organic matter, dispersed on seafloor sediments, and bacterial colonization are consistent and stimulate the development of epifaunal and infaunal bacteria feeder species.

According to all these data, the Bargiano site represents, as first proposed by Baldanza et al. (2013), an accumulation zone of sperm whale carcasses and consequently an environment enriched in organic matter generated by the decay of the carcasses. Further sampling in the studied area could confirm this hypothesis.

In conclusion, marine clay sediments in the Allerona area record three main sperm-whale death events at least, identifiable, at the moment, only by the occurrence of fossilized ambergris cololites.

CONCLUSIONS

The introduction of *Ambergrisichnus alleronae* igen. et isp. nov. increases the knowledge of vertebrate cololites, particularly of marine mammals. The detailed description of cololites, their microstructure, and new mineralogical data confirm the original interpretation of these enigmatic structures as fossil ambergris by Baldanza et al. (2013). In particular, they can be referred to as ambergris cololites, specifically as evisceralites, as indicated by several researchers for modern ambergris origin (Clarke, 1954, 2006; Baynes-Cope, 1962). The large accumulation of cololites is still an unresolved problem. The molluscan fauna exhibits a similarity with whale-fall communities and several lines of evidence document bacterial activity. Three mass-mortalities at least are inferred, associated with whale carcasses sinking in relatively deep water rather than stranding. Unfortunately, these events are identifiable, at the moment, only on the basis of fossilized ambergris. This work, aside from contributing to the advancement of knowledge in the field of ichnology and on the potential for conservation for bioderived substances, offers insights on the spread of odontocetes in the Tyrrhenian Sea during the Pleistocene. Moreover, it opens new scenarios for understanding taphonomic processes, subsequent to whale falls, and the role of bacterial consortia involved in biomineralization and early diagenetic processes in inner-shelf marine environments.

ACKNOWLEDGMENTS

Authors wish to thank the staff of the Department of Physics and Geology of the Perugia University (Mr. L. Bartolucci, Dr. F. Lazzari, and Mr. L. Nicconi), as well as Dr. A. Tulone for the assistance in thin sections images acquisition. We are also grateful to Dr. A.K. Rindsberg (University of West Alabama, Livingston, Alabama) and Dr. A.P. Hunt (Flying Heritage Collections, Everett, Washington) for their precious suggestions.

REFERENCES

Allison, P.A., Smith, C.R., Kukert, H., Deming, J.W., and Bennett, B.A. 1991. Deep-water taphonomy of vertebrate carcasses: a whale skeleton in the bathyal Santa Catalina Basin. *Paleobiology*, 17:78-89.

Ambrosetti, P., Carboni, M.G., Conti, M.A., Esu, D., Girotti, O., La Monica, G.B., Landini, B., and Parisi, G. 1987. Il Pliocene ed il Pleistocene inferiore del bacino del Fiume Tevere nell'Umbria meridionale. *Geografia Fisica e Dinamica Quaternaria,* 10:10-33.

Amstutz, G.C. 1958. Coprolites: a review of the literature and a study of specimens from southern Washington. *Journal of Sedimentary Petrology,* 28:498-508.

Baldanza, A., Bizzarri, R., and Hepach, H. 2011. New biostratigraphic data from the early Pleistocene Tyrrhenian paleocoast (western Umbria, central Italy). *Geologia Croatica,* 64:133-142.

Baldanza, A., Bizzarri, R., Famiani, F., Monaco, P., Pellegrino, R., and Sassi, P. 2013. Enigmatic, biogenically induced structures in Pleistocene marine deposits: a first record of fossil ambergris. *Geology,* 41:1075-1078.

Baynes-Cope, A.D. 1962. Analyses of samples of ambergris. *Nature,* 193:978-979.

Bonaduce, G. and Pugliese, N. 1979. Benthic ostracods as depth indicators. *Rapport de la Commission Internationale pour l'Exploration Scientifique de la Mer Méditerranée,* 25/26:167-169.

Branda, S.S., Gonzalez-Pastor, J.E., Ben-Yehuda, S., Losick, R., and Kolter, R. 2001. Fruiting body formation by *Bacillus subtilis*. *Proceedings of the National Academy of Sciences,* 98:11621-11626.

Bromley, R.G. 1990. *Trace fossils, biology and taphonomy*. Special topics in paleontology, 3. Unwin Hyman, London.

Castanier, S., Le Métayer-Levrel, G., and Perthuisot, J.P. 1999. Ca-carbonates precipitation and limestone genesis-The microbiogeologist point of view. *Sedimentary Geology,* 126:9-23.

Chafetz, H.S. 1986. Marine peloids: a product of bacterially induced precipitation of calcite. *Journal of Sedimentary Petrology,* 56:812-817.

Chin, K., Tokaryk, T.T., Erickson, G.M., and Calk, L.C. 1998. A king-sized theropod coprolite. *Nature,* 393:680-682.

Clarke, R. 1954. A great haul of ambergris. *Nature,* 174:155-156.

Clarke, R. 2006. The origin of ambergris. *The Latin American Journal of Aquatic Mammals (LAJAM),* 5:7-21.

Colalongo, M.L. and Sartoni, E. 1979. Schema biostratigrafico per il Pliocene ed il Pleistocene in Italia. *Contributi Preliminari per la Carta Neotettonica d'Italia,* 251:645-654.

Coles, G.P., Ainsworth, N.R., Whatley, R.C., and Jones, R.W. 1996. Foraminifera and Ostracoda from Quaternary carbonate mounds associated with gas seepage in the Porcupine Basin, offshore western Ireland. *Revista Española de Micropaleontologia,* 28:113-151.

Danise, S. and Dominici, S. 2014. A record of fossil shallow-water whale falls from Italy. *Lethaia*, 47:229-243. doi:10.1111/let.12054.

Danise, S., Dominici, S., and Betocchi, U. 2010. Mollusk species at a Pliocene shelf whale fall (Orciano Pisano, Tuscany). *Palaios,* 25:449-456.

Di Geronimo, I., Messina, C., Rosso, A., Sanfilippo, R., Sciuto, F., and Vertino, A. 2005. Enhanced biodiversity in the deep: Early Pleistocene coral communities from Southern Italy, p. 71-86. In Freiwald, A. and Roberts, J.M. (eds.), *Cold-water Corals and Ecosystems*. Springer-Verlag, Berlin.

Dominici, S., Cioppi, E., Danise, S., Betocchi, U., Gallai, G., Tangocci, F., Valleri, G., and Monechi, S. 2009. Mediterranean fossil whale falls and the adaptation of mollusks to extreme habitats. *Geology,* 37:815-818.

Douglas, S. 2005. Mineralogical footprints of microbial life. *American Journal of Science,* 305:503-525.

Duffin, C.J. 1979. Coprolites: a brief review with reference to specimens from the Rhaetic Bone-beds of England and South Wales. *Mercian Geologist,* 7:191-204.

Faranda, C. and Gliozzi, E. 2008. The ostracod fauna of the Plio-Pleistocene Monte Mario succession (Roma Italy). *Bollettino della Società Paleontologica Italiana,* 47:215-267.

Gaillard, C., Olivero, D., and Chebance, M. 2013. Probable aestivation burrows from the Eocene/Oligocene transition in south-eastern France and their palaeoenvironmental implications. *Palaeoworld,* 22:52-67.

Giannetti, A. and Monaco, P. 2004. Burrow decreasing-upward parasequence (BDUP): a case study from the Lower Jurassic of the Trento carbonate platform (southern Alps), Italy. *Rivista Italiana di Paleontologia e Stratigrafia,* 110:77-85.

Granek, J.A. and Magwene, P.M. 2010. Environmental and genetic determinants of colony morphology in yeast. *PLoS Genet,* 6:1-12.

Guernet, C. and Lethiers, F. 1989. Ostracodes et recherches des milieux anciens: possibilités et limites. *Bulletin de la Societé Géologique de France,* 5:577-588.

Hasiotis, S.T., Platt, B.F., Hembree, D.I., and Heverhart, M.J. 2007. The Trace-Fossil Record of Vertebrates, p. 196-218. In Miller III, W. (ed.), *Trace Fossils: Concepts, Problems, Prospects.* Elsevier, Amsterdam.

Hunt, A.P. 1992. Late Pennsylvanian coprolites from the Kinney Brick Quarry, central New Mexico, with notes on the classification and utility of coprolites. *New Mexico Bureau of Mines and Mineral Resources Bulletin,* 138:221-229.

Hunt, A.P. and Lucas, S.G. 2012a. Classification of vertebrate coprolites and related trace fossils p. 137-146. In Hunt, A.P., Milan, J., Lucas, S.G., and Spielmann, J.A. (eds.), *Vertebrate Coprolites*. New Mexico Museum of Natural History and Science Bulletin 57, Albuquerque.

Hunt, A.P. and Lucas, S.G. 2012b. Descriptive terminology of coprolites and recent feces, p. 153-160. In Hunt, A.P., Milan, J., Lucas, S.G., and Spielmann, J.A. (eds.), *Vertebrate Coprolites*. New Mexico Museum of Natural History and Science Bulletin, 57, Albuquerque.

Hunt, A.P., Chin, K., and Lockley, M.G. 1994. The palaeobiology of vertebrate coprolites, p. 221-240. In Donovan, S.K. (ed.), *The Palaeobiology of Trace Fossils*. Johns Hopkins University Press, Baltimore.

Hunt, A.P., Lucas, S.G., Milàn, J., and Spielmann, J.A., 2012. Vertebrate coprolite studies: status and prospectus, p. 5-24. In Hunt, A.P., Lucas, S.G., Milan, J., and Spielmann, J.A. (eds.), *Vertebrate Coprolites*. New Mexico Museum of Natural History and Science, Bulletin, 57, Albuquerque.

Hurtgen, M.T., Lyons, T.W., Ingall, E.D., and Cruse, A.M. 1999. Anomalous enrichments of iron monosulfide in euxinic marine sediments and the role of H2S in iron sulfide transformations: examples from Effingham Inlet, Orca Basin, and the Black Sea. *American Journal of Science*, 299:556-588.

Johnson, G. 2001. PBS. The Voyage of the Odyssey. Track the Voyage. Kiribati. http://www.pbs.org/odyssey/odyssey/20010208_log_transcript.html (May 2012).

Kearns, D.B., Chu, F., Branda, S.S., Kolter, R., and Losick R. 2005. A master regulator for biofilm formation by *Bacillus subtilis*. *Molecular Microbiology,* 55:739-749.

Linnaeus, C. 1758. *Systema naturae, per regna tria naturae, secundum classes, ordines, genera, species, cum characteribus, differentiis, synonymis, locis. Editio decima*. Imprensis Laurentii Salvii, Holmiae.

Mancini, M., Girotti, O., and Cavinato, G.P. 2004. Il Pliocene ed il Quaternario della Medie Valle del Tevere (Appennino Centrale). *Geologica Romana,* 37:175-236.

Mcallister, J.A. 1985. Reevaluation of the formation of spiral coprolites. *University of Kansas Paleontological Contributions Papers,* 114:1-12.

Monaco, P. 2000. Decapod burrows (*Thalassinoides, Ophiomorpha*) and crustacean remains in the Calcari Grigi, lower Jurassic, Trento platform (Italy), p. 55-57. In Zannato, M.G. (ed.), *1st Workshop on Mesozoic and Tertiary decapod crustaceans.* Studi e Ricerche, Associazione Amici del Museo Civico "G. Zannato", Montecchio Maggiore (Vi), 6 Ott. 2000.

Monaco, P., Caracuel, J.E., Giannetti, A., Soria, J.M., and Yébenes, A. 2007. *Thalassinoides* and *Ophiomorpha* as cross-facies trace fossils of crustaceans from shallow to deep-water environments: Mesozoic and Tertiary examples from Italy and Spain, p. 79-82. In Garassino, A., Feldmann, R.M., and Teruzzi, G. (eds.), *3rd Symposium on Mesozoic and Cenozoic Decapod Crustaceans.* Memorie della Società Italiana di Scienze Naturali e del Museo Civico di Storia Naturale di Milano, Milano, May 23-25, 2007.

Montenegro, M.E., Pugliese, N., and Bonaduce, G. 1998. Shelf ostracods distribution in the italian seas. *Bulletin des centres de Recherches Exploration-Production Elf Memoir,* 20:91-101.

Murray, J.W. 2006. *Ecology and applications of benthic foraminifera*. Cambridge University Press.

Northwood, C. 2005. Early Triassic coprolites from Australia and their palaeobiological significance. *Palaeontology,* 48:49-68.

Naganuma, T., Wada, H., and Fujioka, K. 1996. Biological community and sediment fatty acids associated with the deep-sea whale skeleton at the Torishima Seamount. *Journal of Oceanography*, 52:1-15.

Orphan, V.J., Ussler III, W., Naehr, T.H., House, C.H., Hinrichs, K.U., and Paull, C.K. 2004. Geological, geochemical, and microbiological heterogeneity of the seafloor around methane vents in the Eel River Basin, offshore California. *Chemical Geology*, 205:265-289.

Perrin, B. 2005. How to identify ambergris. http://www.ambergris.fr/identification_of_ambergris.html (June 2012).

Piperno, D.R. and Sues, H.D. 2005. Dinosaurs dined on grass. *Science,* 310:1126-1128.

Prasad, V., Stromberg, C.A.E., Alimohammadian, H., and Sahni, A. 2005. Dinosaurs coprolites and the early evolution of grasses and grazers. *Science,* 310:1177-1180.

Raffi, I. 2002. Revision of the early – middle Pleistocene calcareous nannofossil biochronology (1.75-0.85 Ma). *Marine Micropaleontology,* 45:25-55.

Rio, D., Raffi, I., and Villa, G. 1990. Pliocene-Pleistocene calcareous nannofossil distribution patterns in the western Mediterranean, p. 513-533. In Kastens, K. and Mascle, J. (eds.), *Proceeding Ocean Drilling Program Scientific Results*, 107. College Station, Texas.

Sagemann, J., Bale, S.J., Briggs, D.E.G., and Parkes, R.J. 1999. Controls on the formation of authigenic minerals in association with decaying organic matter: an experimental approach. *Geochimica and Cosmochimica Acta,* 63:1083-1095.

Salman, V., Armann, R., Girnth, A., Polerecky, L., Bailey, J.V., Hogslund, S., Jessen, G., Pantoja, S., and Schultz-Vogt, H.N. 2011. A single cell sequencing approach to the classification of large vacuolated sulfur bacteria. *Systematic and Applied Microbiology,* 34:243-259.

Sciuto, F. 2005. Ostracodi batiali pleistocenici di Capo Milazzo (Sicilia NE) ed implicazioni paleoambientali. *Rendiconti della Società Paleontologica Italiana,* 2:219-227.

Shapiro, R.S. and Spangler, E. 2009. Bacterial fossil record in whale-falls: Petrographic evidence of microbial sulfate reduction. *Palaeogeography, Palaeoclimatology, Palaeoecology*, 274:196-203.

Shelton, C.D. 2013. A new method to determine volume of bromalites: morphometrics of Lower Permian (Archer City Formation) heteropolar bromalites. *Swiss Journal of Palaeontology,* 132:221-238.

Smith, C.R. and Baco, A.R. 2003. Ecology of whale falls at the deep-sea floor. *Oceanography and Marine Biology: An Annual Review,* 41:311-354.

Smith, C.R., Baco, A.R., and Glover, A. 2002. Faunal succession on replicate deep-sea whalefalls: Time scales and vent-seep affinities. *Cahiers de Biologie Marine,* 43:293-297.

Southam, G., Ravin, D., Rostad, A., and Brock, C. 2001. Pyrite discs in coal: evidence for fossilized bacterial colonies. *Geology,* 29:47-50.

Spencer, P.K. 1993. The "coprolites" that aren't: The straight poop on specimens from the Miocene of southwestern Washington State. *Ichnos,* 2:231-236.

Stewart, J.D. 1978. Enterospirae (fossil intestines) from the Upper Cretaceous Niobrara Formation of western Kansas. *University of Kansas Paleontological Contributions Papers,* 89:9-16.

van de Schootbrugge, B., Harazim, D., Sorichter, K., Oschmann, W., Fiebig, J., Püttmann, W., Peinl, M., Zanella, F., Teichert, B.M.A., Hoffmann, J., Stadnitskaia, A., and Rosenthal, Y. 2010. The enigmatic ichnofossil *Tisoa siphonalis* and widespread authigenic seep carbonate formation during the late Pliensbachian in southern France. *Biogeosciences,* 7:3123-3138.

Van Lith, Y., Warthmann, R., Vasconcelos, C., and McKenzie, J.A. 2003. Microbial fossilization in carbonate sediments: a result of the bacterial surface involvement in dolomite precipitation. *Sedimentology,* 50:237-245.

Vasconcelos, C. and McKenzie, J.A. 1997. Microbial mediation of modern dolomite precipitation and diagenesis under anoxic conditions (Lagoa Vermelha, Rio de Janeiro, Brazil). *Journal of Sedimentary Research,* 67:378-390.

Vasconcelos, C., McKenzie J.A., Bernasconi, S., Grujic, D., and Tien, A. J. 1995. Microbial mediation as a possible mechanism for natural dolomite formation at low temperature. *Nature,* 377:220-222.

Vogt, W., 2011. Ambergris photo. William Vogt photos at pbase.com. http://www.pbase.com/wvphoto/image/37569744 (June 2012).

Warthmann, R., Van Lith, Y., Vasconcelos, C., McKenzie, J.A., and Karpoff, A.M. 2000. Bacterially induced dolomite precipitation in anoxic culture experiments. *Geology,* 28:1091-1094.

Wright, D. 1999. The role of sulphate-reducing bacteria and cyanobacteria in dolomite formation in distal ephemeral lakes of the Coorong region, South Australia. *Sedimentary Geology,* 126:147-157.

Williams, M.E. 1972. The origin of spiral coprolites. *University of Kansas Paleontological Contribution,* 59:1-12.

Zopfi, J., Böttcher, M., and Jørgensen, B.B. 2008. Biogeochemistry of sulfur and iron in *Thioploca*-colonized surface sediments in the upwelling area of central Chile. *Geochimica and Cosmochimica Acta,* 72:827-843.